LONG-PERIOD SURFACE-WAVE EFFECTS ON FLEXIBLE BRIDGE STRUCTURES

WANG Tao, CHEN Jie, WANG Haiyun

Institute of Engineering Mechanics, China Earthquake Administration

June 6, 2026
ChangSha, China

00| Content

Numerous Bridges

Changtai bridge

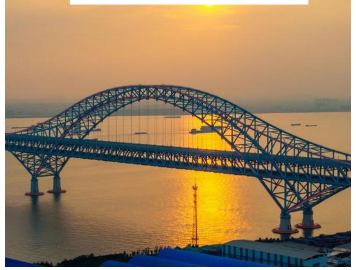

CZ Railway

Shen-zhong bridge

Beipanjiang bridge

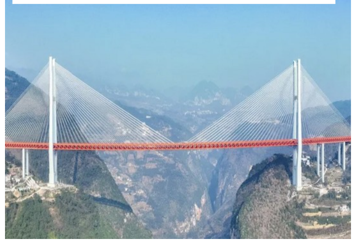

Serious EQ risk

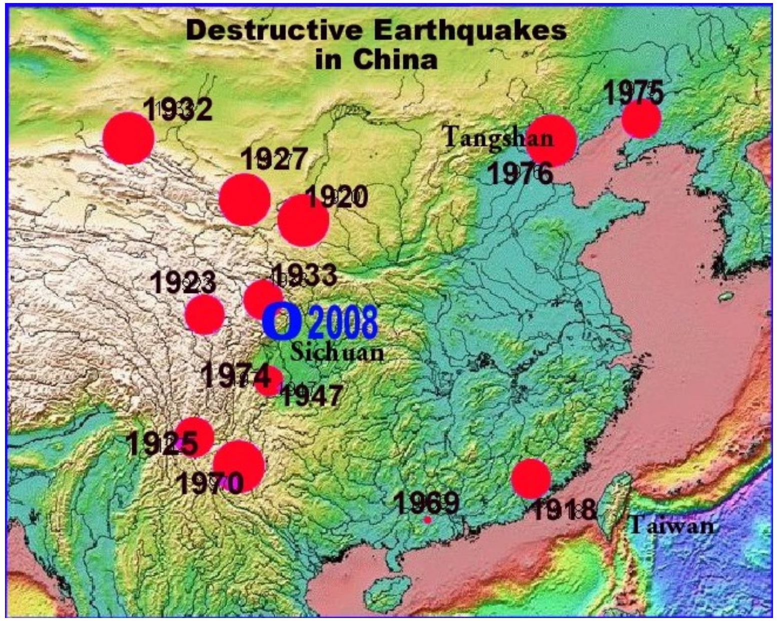

Critical consequence

Seismic safety of major bridges is critical to traffic lifeline continuity. Systematic seismic performance evaluation is strategically important.

Multiple factors influence bridge seismic response

Site effect

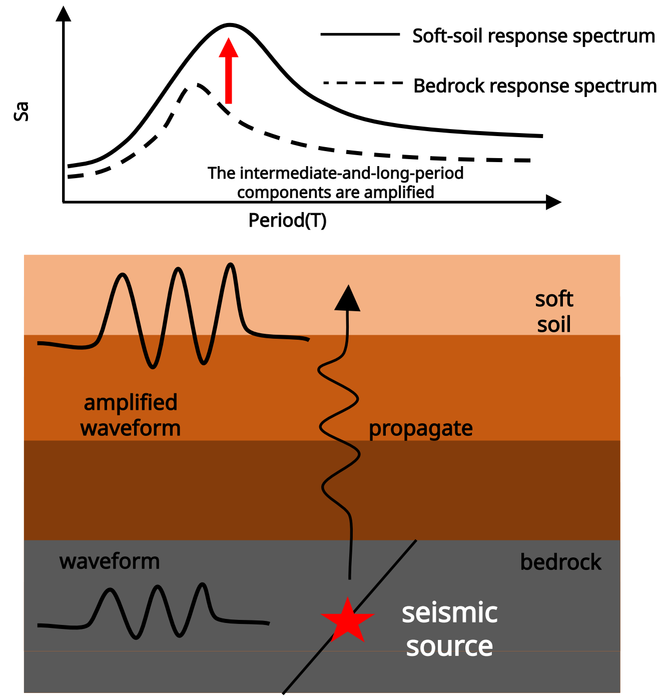

The soft soil layer has a significant amplification effect on ground motion

Waveform characteristic

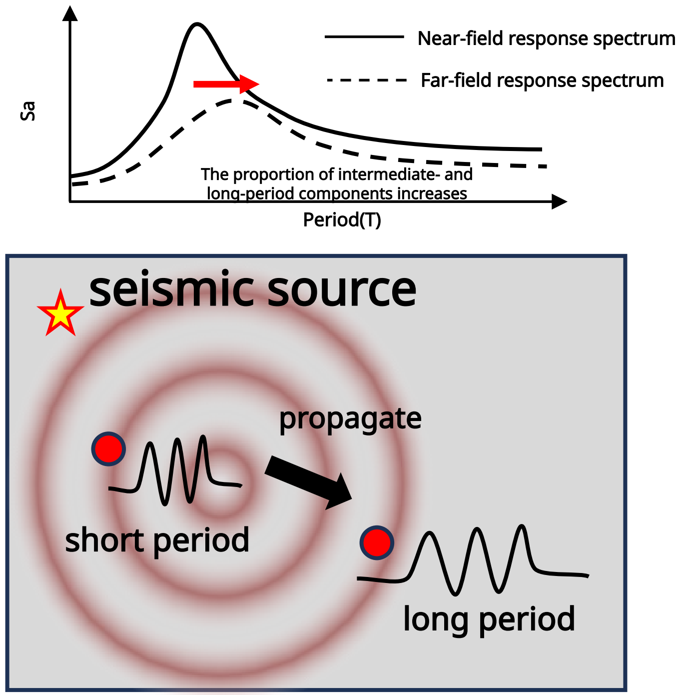

Surface waves, with long periods, slow attenuation and high energy, seriously threaten long-span bridges

Structural system

Bridge geometry, stiffness and connection details directly determine structural seismic survival probability

■ Potential Impact of Surface Waves on Flexible Bridges

- Slow attenuation
- Long-period characteristic
- Long duration

- Resonance Effect
- Traveling Wave Effect
- Cumulative Damage

Typical Case: 2011 Great East Japan Earthquake ——This earthquake recorded over 2-minute multi-pulse long-duration surface wave motions, causing extensive cumulative damage to coastal long-span bridges and providing a typical surface wave damage sample.

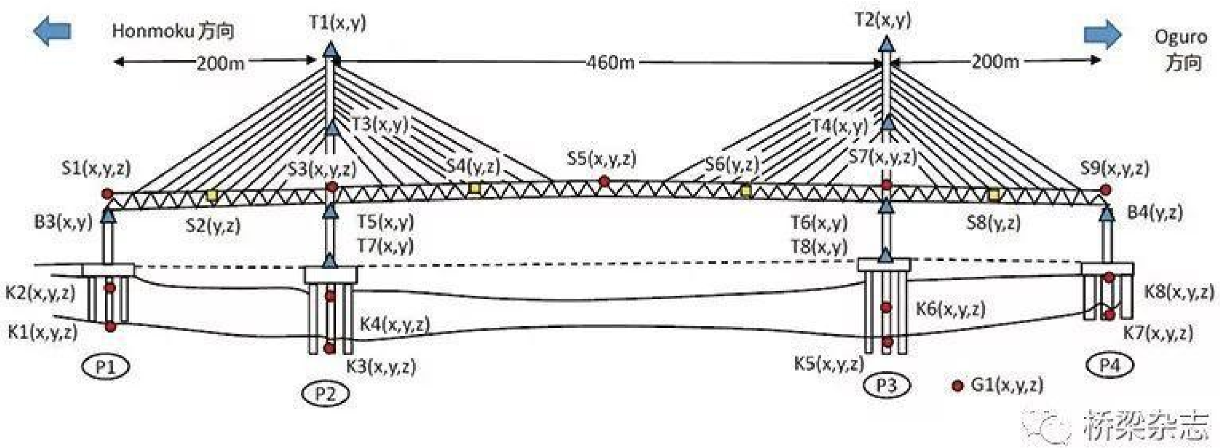

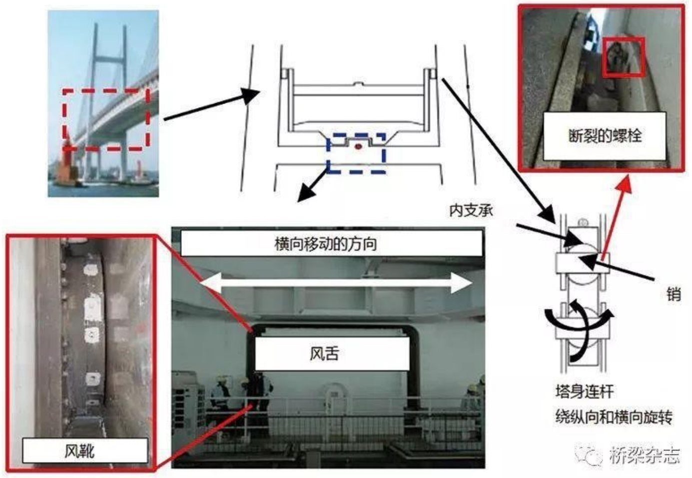

@ Tomoaki Takeda, IABSE SYMPOSIUM NANTES 2018

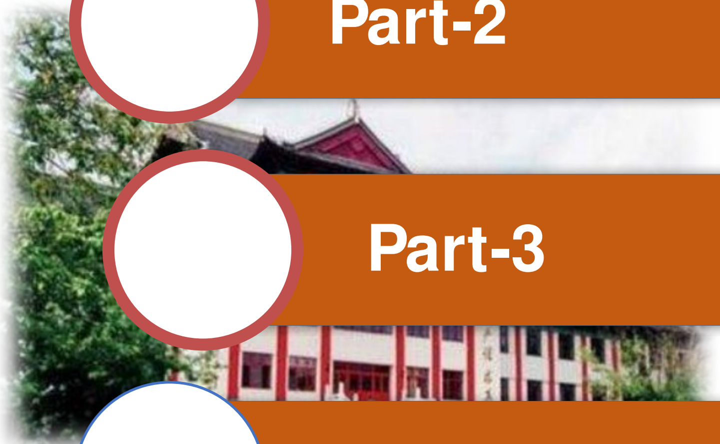

Existing Surface Wave Extraction Methods

Traditional Extraction Methods

•**Frequency-domain Filtering:** Relies on **frequency differences** for separation. In the long-period wave band, the time-frequency ranges of surface waves, body waves, and coda waves highly overlap, and simple filtering will lead to signal distortion.

•**Spatial Wavenumber Method (F-K/Array)**： Relies on array spatial gradient calculation. It requires dense station to obtain **wavenumber** characteristics, and fails in single-station observation due to lack of spatial constraints.

Three-component Polarization Identification Method

•**Core Logic**: Fully exploit the particle motion trajectory characteristics (such as **polarization** rate, **ellipse major axis deflection**, etc.) of single-station three-component (3C) records to realize wavefield decoupling at the physical level.

•**Motion Trajectory Constraint:** Utilize the elliptical polarization characteristics of Rayleigh waves to identify target components from noisy signals through mathematical transformation.

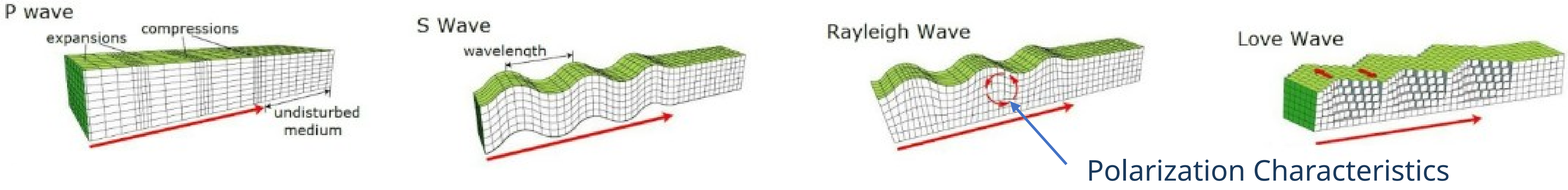

Limitations of Existing Methods and Rayleigh-like Deflection Problem

Instability of Traditional Methods

- **Fixed R-V Orthogonal Phase Selection**

  Classifies the deflected Rayleigh-like energy as "insufficiently Rayleigh", leading to missed detection.

- **Single Reference Azimuth Projection**

  Projects the target energy onto incorrect R/T/V components.

- **Over-simplified Interpretation**

  Directly interprets deflection or transverse participation as Love waves, resulting in over-simplification.

Physical Mechanism of Deflection

Real Rayleigh-like long-period waves do not necessarily maintain an ideal fixed R/V ellipse:

- Local changes in propagation direction
- 3D medium effects
- Scattering / conversion
- Transverse participation

All the above factors may cause the local ellipse to deflect relative to the fixed R/V axes.

Single-station Extraction of Long-period Surface Wave

Main Challenges

- ▶ Single station lacks spatial array constraints, making direct wave decomposition unreliable or impossible
- ▶ Rayleigh-like, Love-like and scattered waves can overlap within the same time-frequency range
- ▶ Even for a target Rayleigh-like wave packet, **the propagation azimuth and principal axis of the R-V ellipse may also be locally deflected**

Extraction Method

A surface wave extraction method **based on propagation consistency (PCE)** is proposed to extract interpretable long-period surface wave components and identify their spatial orientation

Total Wavefield Composition

Original Total Wavefield = Rayleigh Component + Love Component + Quasi-standing Wave Component + Mixed Residuals

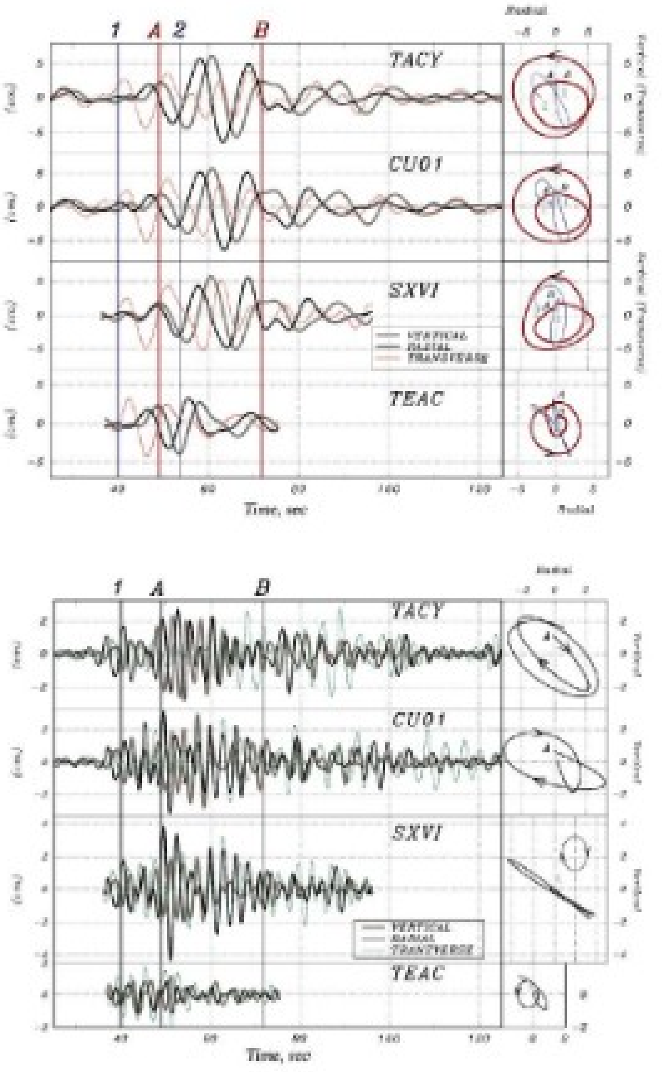

ig. 12. Displacements at stations TACY, CU01, SXVI, and TEAC passband filtered at 0.063–0.15 Hz (above) and 0.2–0.3 Hz (I
Extracted particle motion (right side), after Gómez-Bernal (2002).

Limitations of Existing Methods and Rayleigh-like Deflection Problem

PCE Solution Approach： **Propagation Angle Identification** → Local Axis Time-frequency Domain → Surface Wave Major Axis Constraint→ Propagation Consistency Constraint

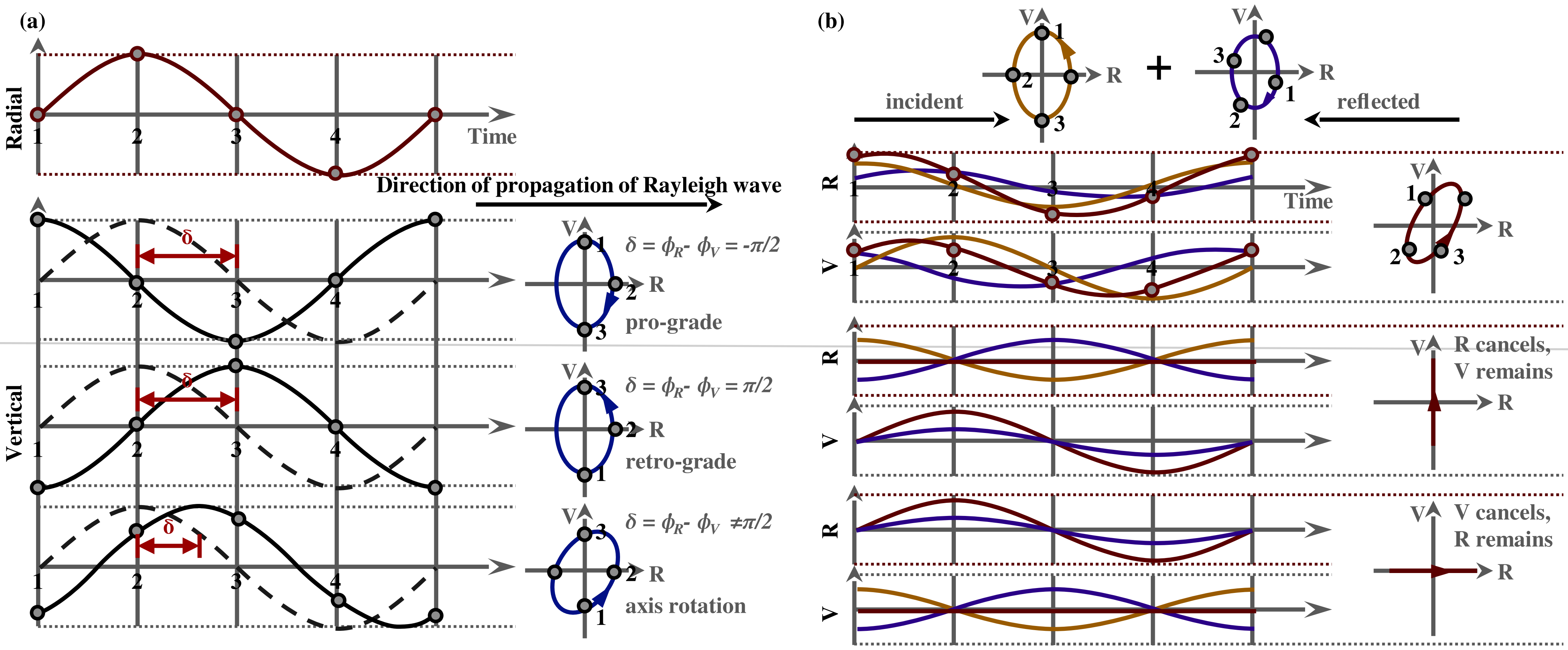

- Mechanism of Particle Motion Axis Deflection and Superposition with Quasi-standing Wave Patterns

Overall Process

Three-layer Extraction

- **Rayleigh-like:** Retain propagation-consistent in-plane R-V energy with local major axis deflection
- **Love-like:** Get transverse long-period energy in the Rayleigh residual
- **Standing-like:** Set the window for quasi-standing wave pattern or merged residual

Theoretical Derivation of Major Axis Inclination

- Under ideal elastic and laterally homogeneous medium

$$\frac{S_V}{S_R} = -i\frac{G}{F}$$

  - The radial and vertical components satisfy an approximate phase difference of ±90°.
  - The major axis of the ellipse is usually aligned with the radial (R) or vertical (V) direction.
  - The real part of the covariance matrix (cross-spectrum) is zero under ideal conditions.

- Major axis deflection in non-ideal media
  - **Complex eigenfunctions:** In anelastic dissipative media, the eigenfunctions F and G become complex numbers.
  - **Phase deviation:** The phase difference is no longer equal to ±90°, leading to a major axis tilt $\psi \neq 0$.
  - **Calculation formula:**

$$\tan 2\psi = \frac{2\,|S_R|\,|S_V|\cos\delta}{|S_R|^2 - |S_V|^2}$$

Time-frequency Representation and Local Azimuth Estimation

➢ **Core Principle：** PCE starts from local R, T, V representations, rather than a fixed global radial direction.

- **Step 1 — Stockwell Transform**

  Obtain the three-component complex time-frequency field $S(\tau,f) = [S_N, S_E, S_V]^T$

- **Step 2 — Local Azimuth Estimation**

  Estimate the local propagation-related azimuth per time-frequency cell:

  $$\theta_{TF}(\tau,f) = \operatorname{argmax}_\theta \, |\cos\theta \cdot S_N + \sin\theta \cdot S_E|$$

- **Step 3 — Time-frequency Rotation**

  Rotate the horizontal components to local R/T coordinates:

  $$[S_R, S_T, S_V]^T = R(\theta_{TF}) \, [S_N, S_E, S_V]^T$$

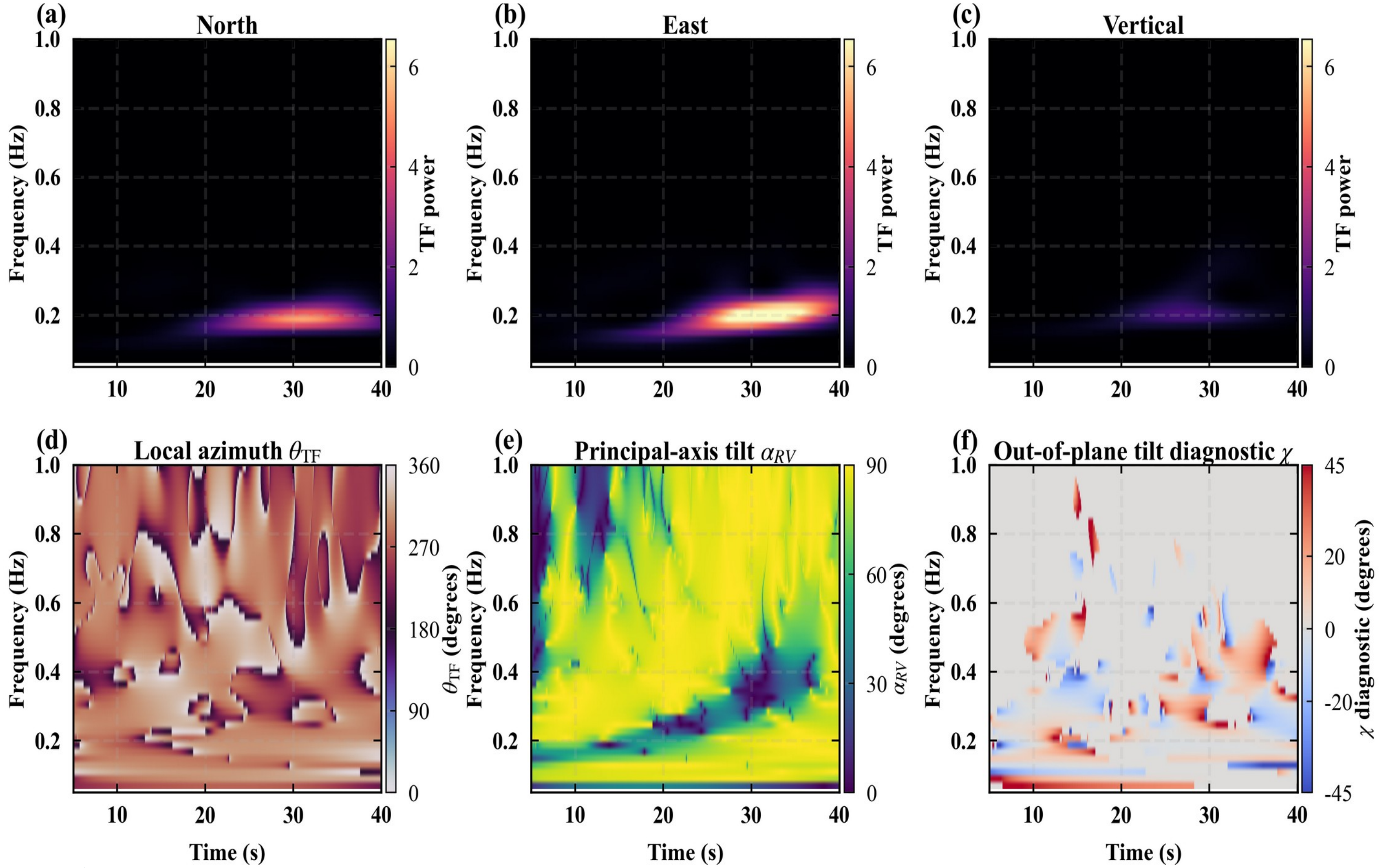

➢TCU118 three-component time-frequency power spectra (top) and local diagnostic parameters (bottom)

➢ **Triple Roles of Local Azimuth θ_TF：**

▶ For local coordinate construction (R/T rotation)

▶ As a diagnostic parameter for propagation azimuth

▶ **Provides spatial consistency constraints for subsequent PCE masking**

Local Major Axis Correction and PCE Mask Construction

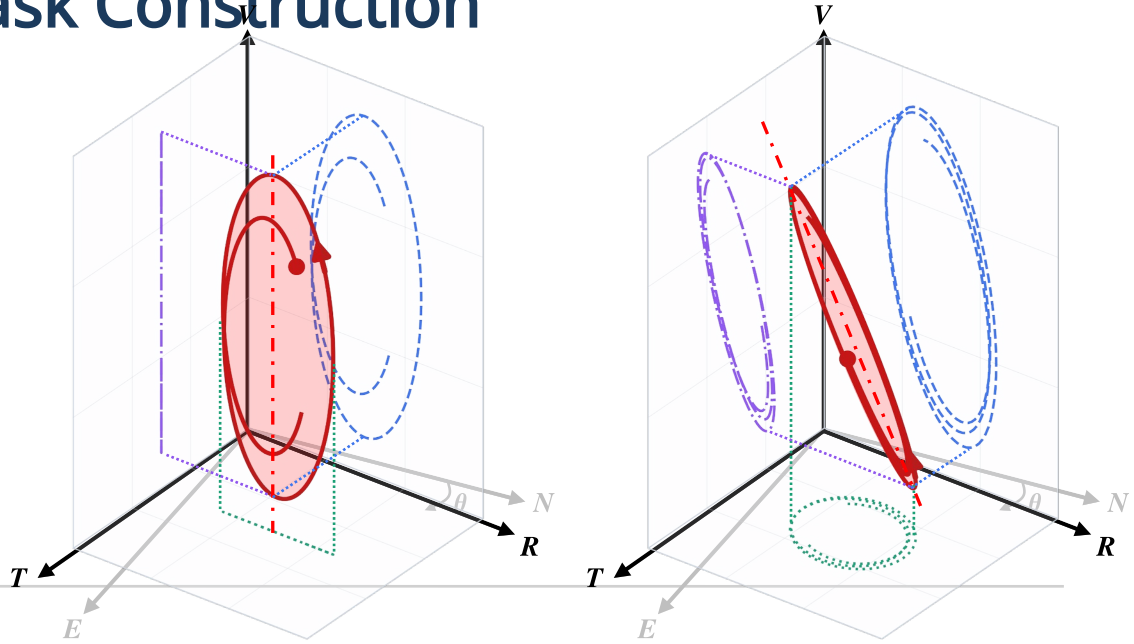

Local Major Axis Correction

Estimate local major axis direction ψ(τ,f) in the R-V plane, correct the observed tilt, and avoid missing tilted Rayleigh-like energy due to the fixed R-V orthogonal assumption.

$$\psi(\tau,f) = \tfrac{1}{2}\,\mathrm{atan2}\left(2\mathrm{Re}(S_R \cdot S_V^*),\ |S_R|^2 - |S_V|^2 \right)$$

$$S_{maj} = \cos\psi \cdot S_R + \sin\psi \cdot S_V \qquad \alpha_{RV} = 90^\circ - |\psi|$$

PCE Propagation Consistency Mask

$$M_{PCE} = M_{phase} \cdot M_{rot} \cdot M_{sync} \cdot M_{env} \cdot M_{TF}$$

M_{phase}: R-V phase relationship satisfies Rayleigh-like candidates

M_{rot}: Clear local sense of rotation, distinguishing retro/pro-grade candidates

M_{sync}: Synchronization of major/minor axis structure

M_{env}: Co-occurrence of R and V envelopes

M: Time-frequency continuity and connectivity filtering

Output Formula

$$u_{Rayleigh}^{PCE} = S^{-1}(M_{PCE} \cdot S_{RV})$$

Primary Features of PCE

▶ Not a single threshold, but a set of local phase, rotation, and continuity constraints

▶ Constructs a continuous time-frequency mask by integrating multiple physical indicators

▶ Determines the surface wave region through connectivity screening

PCE Constraint Indicator Parameter System

Indicator Name	Symbol	Default Value	Core Function
Phase Consistency	Cϕ,0	0.60	Judge whether the phase relationship is stable within a short time window
Rotation Ambiguity	Aamb,0	0.35	Suppress rotation cancellation or overlapping windows (quasi-standing wave identification)
Major-Minor Axis Synchronization	Dv,0	0.30	Judge whether the frequencies of Major/Minor components are consistent
Envelope Co-occurrence	E0	0.20	Require two axial components to appear synchronously in the time domain
In-plane Dominance (IP)	η0	0.92	Strict screening for the conservative subset of PCE-IP

➢ Parameter Design Logic

▶ **Phase Consistency (0.60)** is the highest-weight indicator, ensuring stable Rayleigh-like phase relationships.

▶ **Rotation Ambiguity (0.35)** is used to identify quasi-standing wave windows — rotation cancellation indicates bidirectional interference.

▶ **In-plane Dominance (0.92)** is the strictest threshold, retaining only a conservative subset with highly in-plane polarization.

▶ The five indicators jointly form a hierarchical screening system that converges gradually from loose to strict.

Local Polarization Diagnosis and Love-like Transverse Extraction

Local Polarization Geometric Diagnostic Parameters

- **In-plane Major Axis Angle $\alpha_{RV} = 90° - |\psi|$**
  Describes the deflection of the major axis within the R-V plane.
- **Out-of-plane Tilt Angle χ**
  Describes the lateral offset of the dominant polarization direction relative to the propagation plane.
- **Degree of Polarization DoP**
  Evaluates the uniqueness of the polarization state via eigenvalue decomposition.

Window State Classification

Resolvable	Ambiguous	Merged	Unresolved

- **Diagnostic Principle:** Resolvable windows report full attitude parameters (θ_{TF}, α_{RV}, χ); unresolvable windows retain state labels (Ambiguous/Merged/Unresolved)
- **Love-like Localization：** Not an independent Love wave mode separation, but a transverse long-period supplement in the Rayleigh residual, which together with PCE Rayleigh-like forms the main package

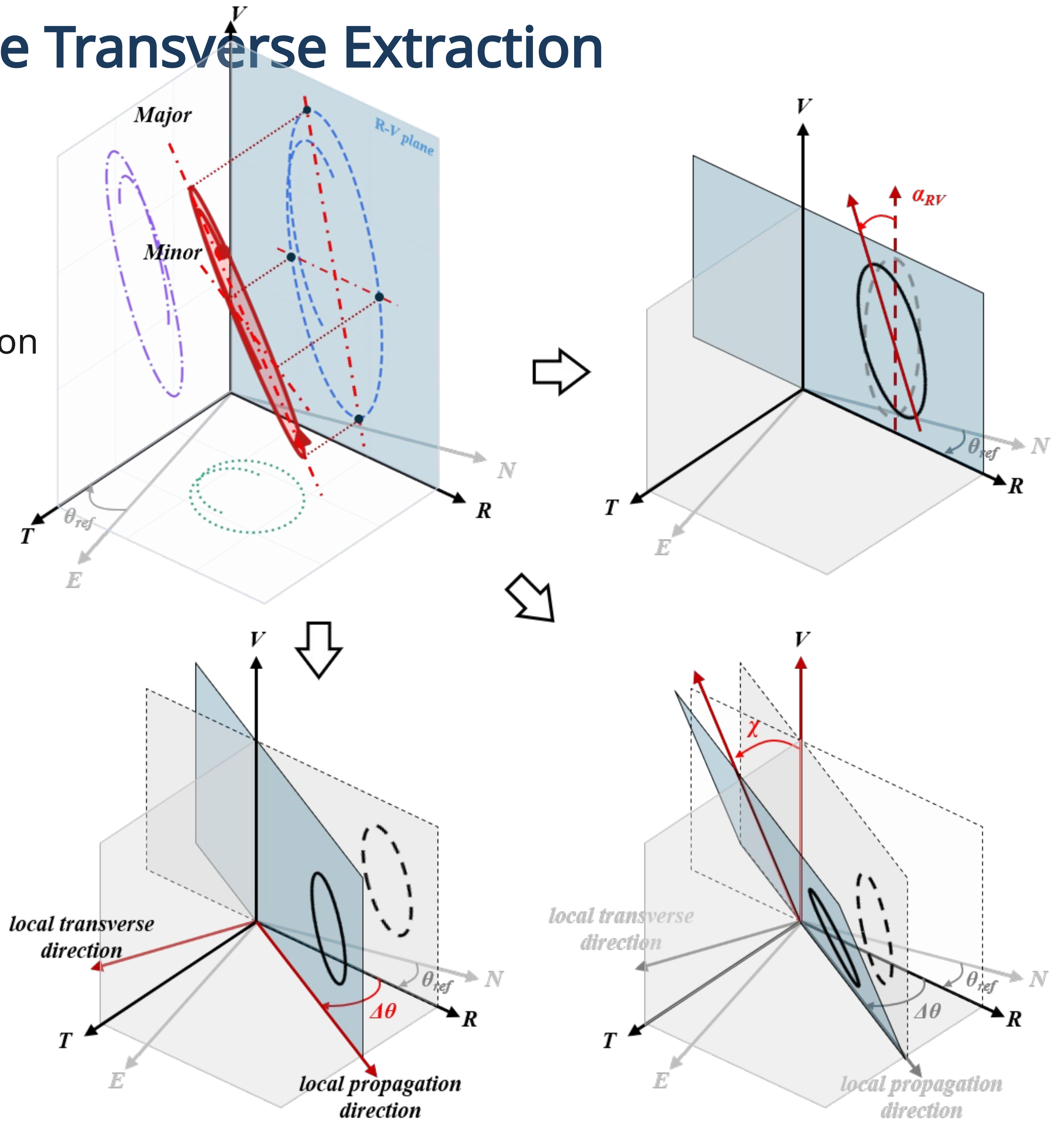

Output Hierarchy of Main Package and Extended Package

Main Package — Primary Extracted Long-period Surface Wave Packet

Composition: PCE Rayleigh-like + PCE Love-like

- Emphasizes propagation consistency and rotation clarity
- Core product of the main extraction workflow
- Retains propagation-consistent long-period surface wave-related energy
- Do not force all low-frequency residuals to be interpreted as surface waves

Extended Package — Extended Long-period Surface Wave Packet

Composition: Main Package + structured residual long-period candidate windows

- Incorporates candidate windows with quasi-standing wave or merged characteristics
- Provides a broader physical perspective for basin effect research
- Aids in result interpretation, not a new propagation branch
- Not a rigorous proof of standing waves

➢ TCU118

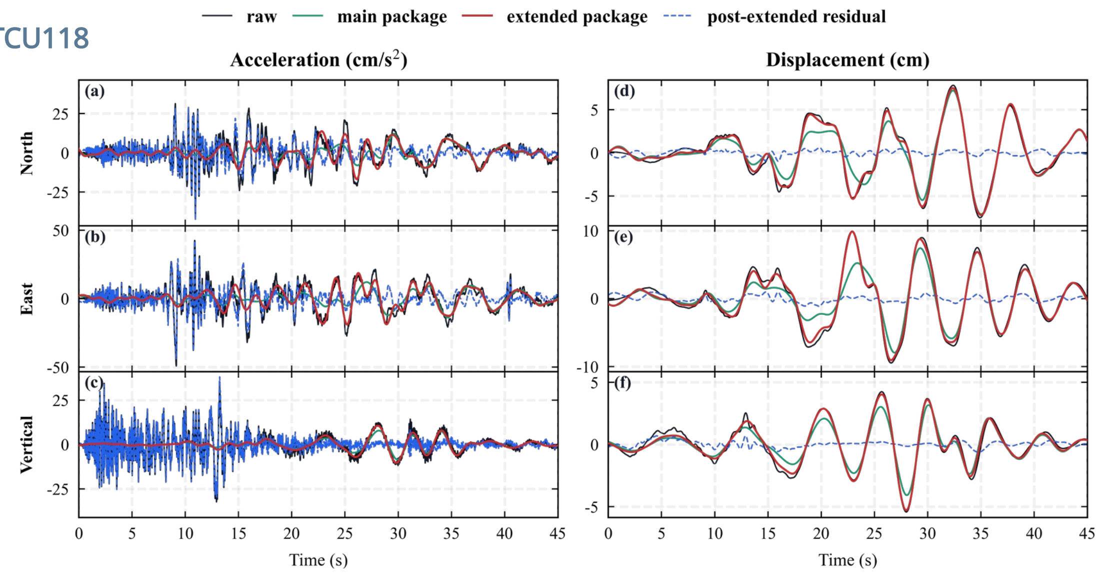

➢ **Extended package:** An auxiliary interpretation :

- It is not a new independent propagation branch
- Nor is it a rigorous proof of standing waves
- Requires multi-station spatial verification

Identification of candidate windows for quasi-standing-wave components

Standing-like localization:

Single-station residual candidates ≠ strict standing-wave proof；
Bidirectional interference/rotational cancellation judged via retro/pro energy matching

$$I_{stand,m} = 2 \cdot \min(E_{retro,m}^{res}, E_{pro,m}^{res}) / (E_{retro,m}^{res} + E_{pro,m}^{res} + \varepsilon)$$

TCU118 vs TCU116 Comparison:

- TCU118: Obvious in-plane axis deflection, rich residual candidate windows
- TCU116: Concentrated long-period main energy, few residual candidate windows
- Both sites verify Standing-like's auxiliary explanatory

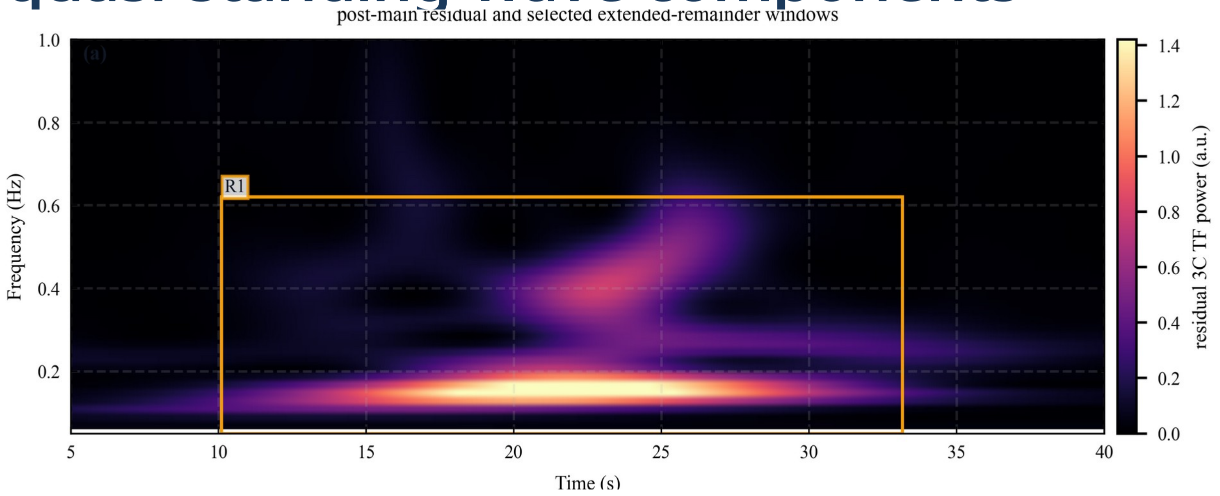

TCU118 post-main residual Time-frequency diagram
(marking of R1 candidate windows）

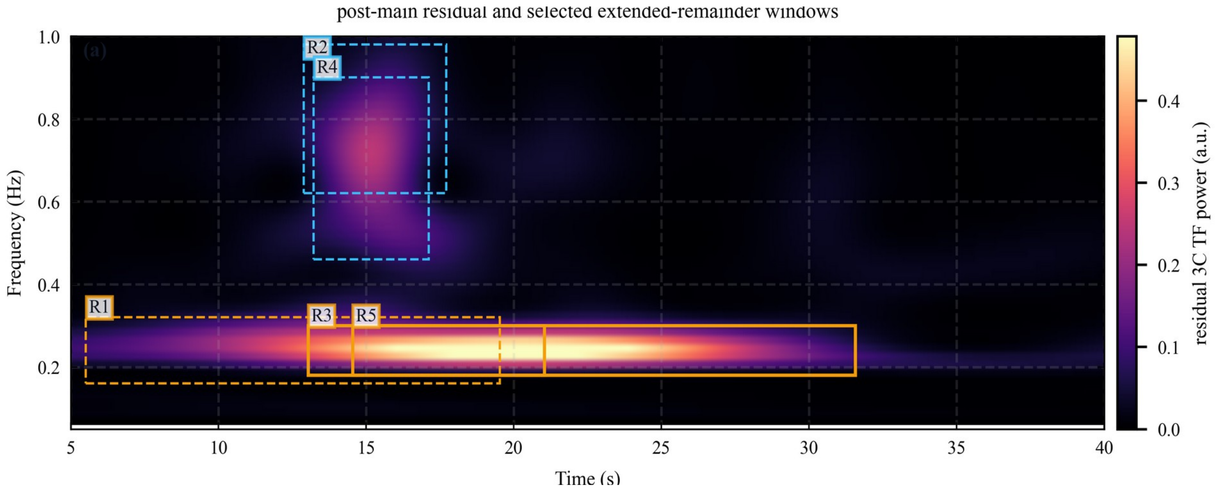

TCU116 post-main residual Time-frequency diagram

Validation with observational records: TCU118

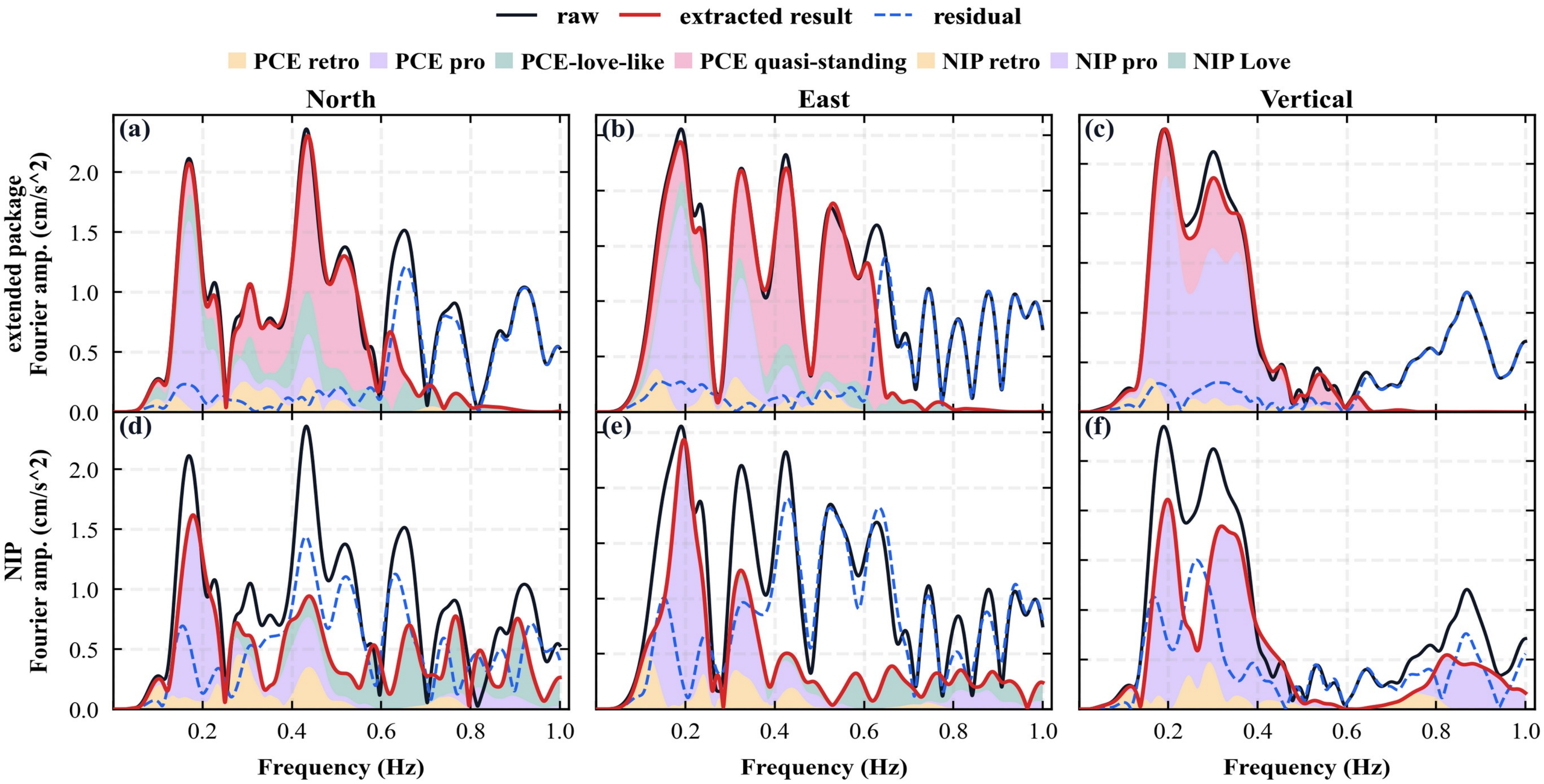

➢ TCU118 PCE vs NIP Spectral decomposition comparison(extended package / Normalized Inner Product (NIP))

▶ Marked in-plane principal axis deflection

▶ Love-like effectively identified

Contrast of TCU116 and comparison with NIP method

➢ TCU116 as a relatively stable control case

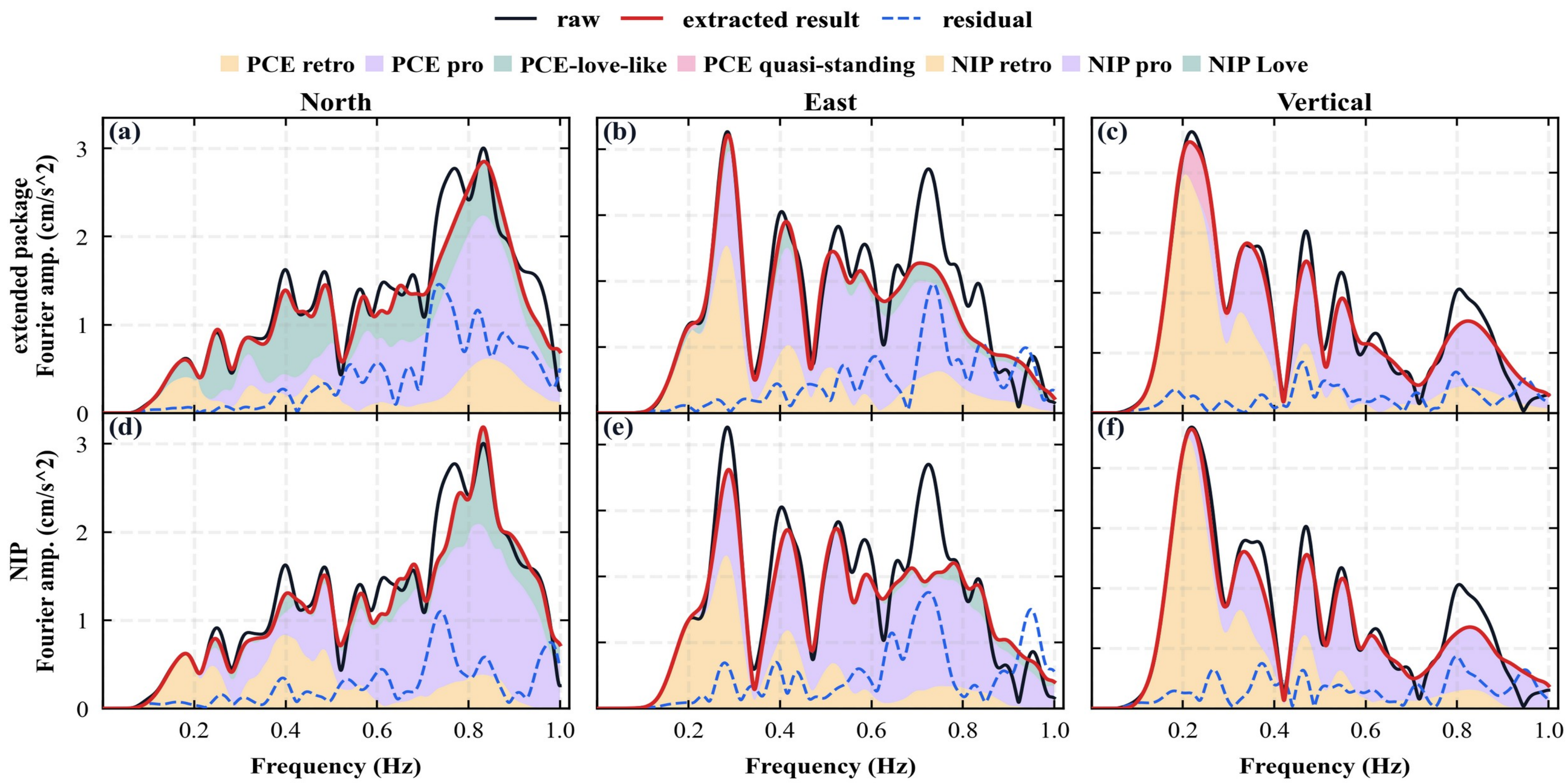

➢ TCU116 PCE vs NIP Comparison of spectral decomposition results

▶ Long-period energy largely concentrated

▶ Few residual candidate windows enter extended margin

▶ Overall still close to dominant wave-packet interpretation

Contrast of TCU116 and comparison with NIP method

Comparison between PCE and NIP methods

- NIP: more oriented to fixed-component correlation/rotational decomposition
- PCE: introduce corrections for local propagation azimuth and principal axis
- PCE: deliver hierarchical output and diagnostic capability

Comparison dimensions	NIP	PCE
Decomposition logic	Fixed-component correlation / rotational decomposition	Local propagation azimuth plus principal axis correction
Rayleigh	retro + pro	Rayleigh-like + diagnostics
Love	NIP-linear / Love-like	PCE Love-like
Residual	No extended interpretation	With extended remainder

Interpretation of Boundaries and Method Localization

Resolvable Windows

Local windows featuring stable support and adequate concentration report complete waveform attitude：

- θ_{TF} — Local Propagation Azimuth
- α_{RV} — In-Plane Principal Axis Angle
- χ — Out-of-Plane Offset Angle

Unresolvable Windows

Retain status marks in cases of severe overlap or rotational cancellation：

- ambiguous
- merged
- unresolved

Quasi-Standing-Wave Candidates

Standing-like residual requires additional verification：

- Requires multi-station spatial validation.
- Only for auxiliary interpretation.

Method Localization

The framework of this study is not a complete modal decomposition; instead, it yields constrained, diagnosable, well-bounded long-period surface wave extraction under the single-station condition

▶ It hierarchically isolates interpretable components associated with long-period surface waves and explicitly defines their interpretation boundaries

▶ Report waveform attitudes **only for resolvable windows**; retain status labels and candidate constraints for unresolvable segments

▶ All interpretations of residuals are marked as candidates to avoid excessive mechanistic judgment

00| Content

03| Dynamics of Shuanghe Cable-stayed bridge

- **The Shuanghe Extra-large Bridge** in Qiaojia County, Zhaotong City is the **controlling project** of the Huiqiao Expressway. **It is a composite girder cable-stayed bridge with high-low pylons, with a total length of 705.6 m.**

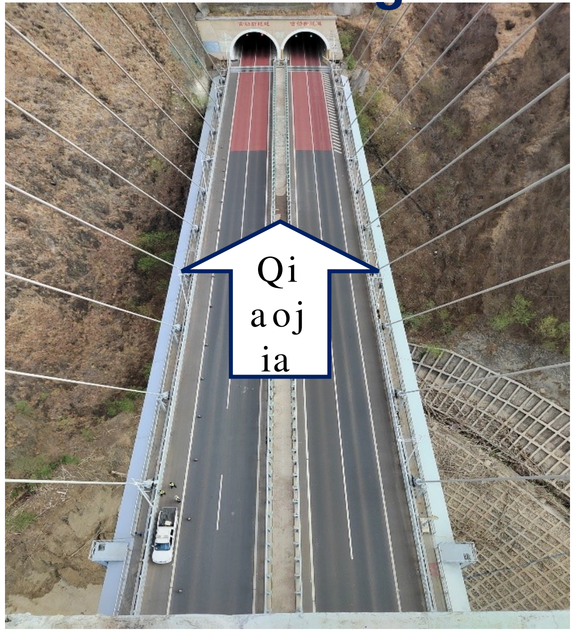

- **Bridge type:** Composite girder cable-stayed bridge with twin pylons, double cable planes and high-low pylons;
- **Total length and span:** Total length ≈ 705.6 m, main span ≈ 356 m;
- **Pylon height:** Pylon 2 ≈ 229 m, Pylon 3 ≈ 170 m;
- **Deck width:** ≈ 28.7 m;
- **Deck height:** Deck elevation ≈ 190 m above the Shuanghe valley bottom;
- **Highway class:** Four-lane two-way expressway, design speed 80 km/h;
- **Design load:** Highway Class-I;
- **Seismic fortification:** Seismic fortification intensity 8 degrees, peak ground acceleration 0.20g (extracted from public codes for Qiaojia area;
- **Site environment**: Deep canyon landform in the Baihetan Reservoir area of Jinsha River, adjacent to the northern segment of the Xiaojiang Fault Zone, with strong regional seismic activity.

Seismic Environment

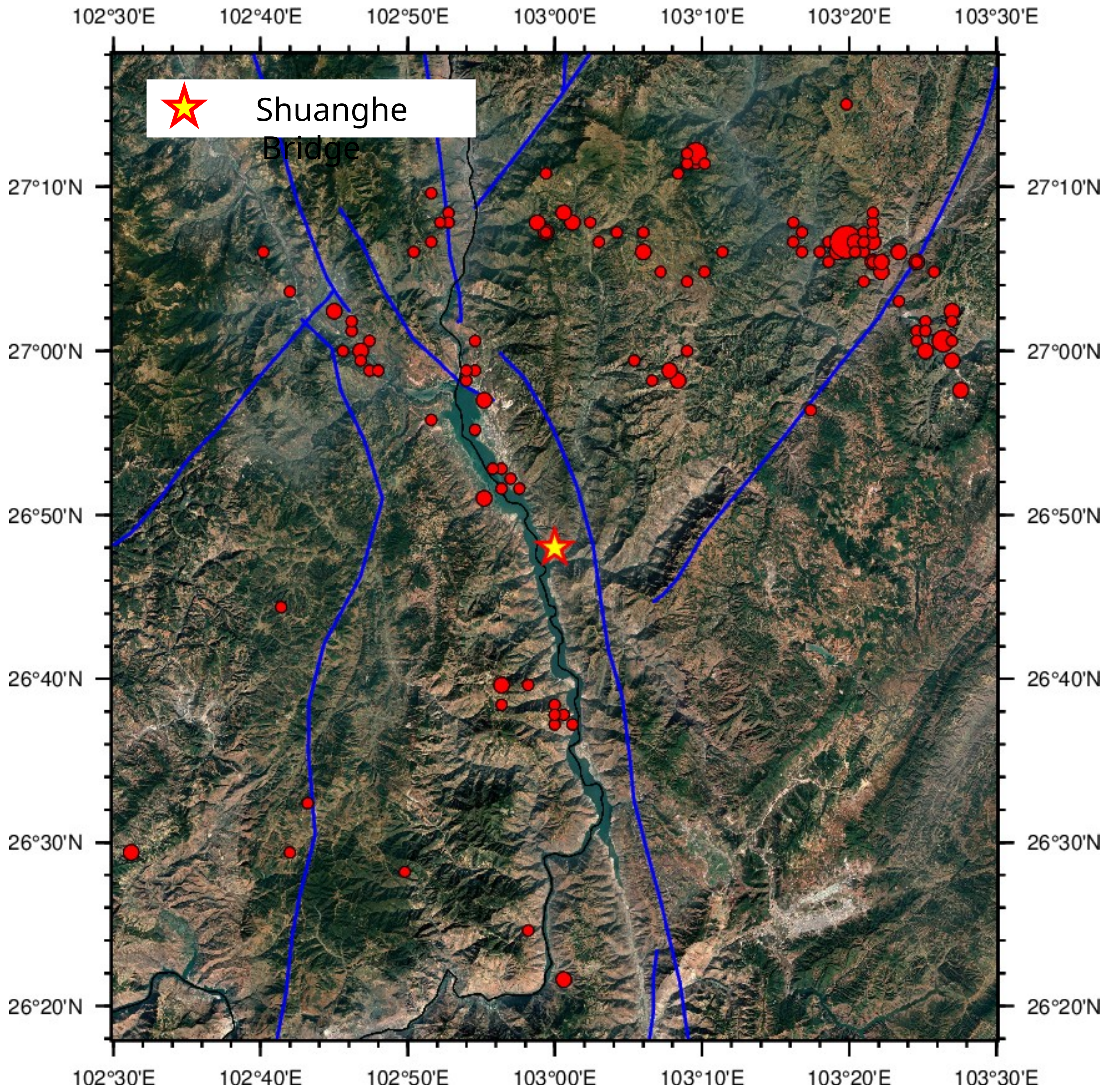

Fault Strike and Historical Earthquake Distribution Around Shuanghe Bridge

Fault Zones：

- The bridge site is located in Jintang Town, Qiaojia County, within a deep canyon landform area of the Baihetan Reservoir on the Jinsha River；
- Influenced by the northern segment of the Xiaojiang Fault Zone and the Sichuan-Yunnan active tectonic system;
- The Shuanghe Extra-large Bridge lies on the Xiaojiang Fault Zone, resulting in frequent regional seismic activity;

Historical Earthquakes：

- The 1733 Dongchuan M7.75 earthquake and the 1850 Xichang M7.5 earthquake resulted in a maximum impact intensity of approximately 8 degrees at the dam site；
- Recent local moderate shocks: 2020 Qiaojia M5.0, 2022 Baihetan M4.2, 2026 Qiaojia M5.1
- The regional seismic risk is characterized by "impacts from strong peripheral earthquakes + frequent moderate and small near-field earthquakes".

Schematic Diagram of Measuring Point Layout Scheme

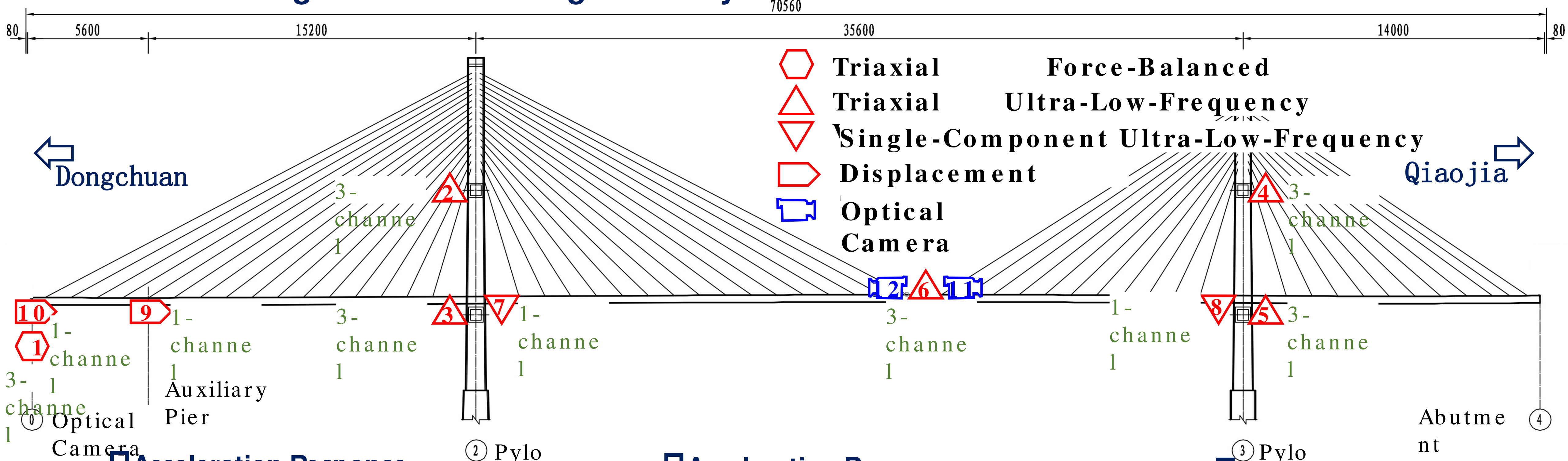

Acceleration Response Monitoring at Pylon Top

Acceleration Response Monitoring at Pylon Base

Deck Acceleration Response Monitoring

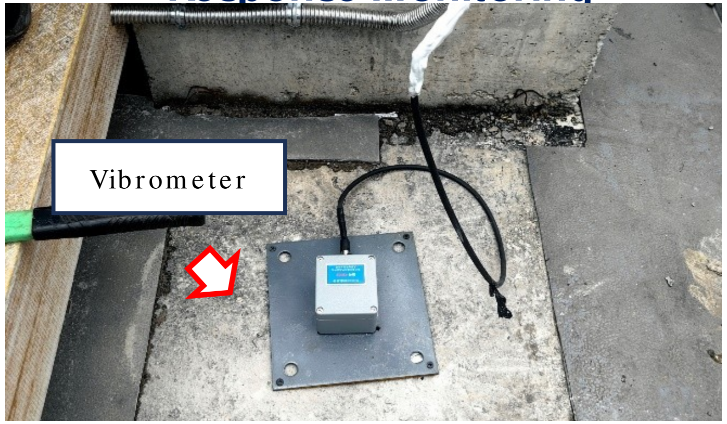

03| Dynamics of Shuanghe Cable-stayed bridge

■Seismic Event ——M3.0 Earthquake in Qiaojia County

Origin Time： 2024-06-14 06:02:28
Latitude： 27.01°N
Longitude： 103.40°E
Depth： 10km
Magnitude： M3.0
Hypocenter Location： Qiaojia County, Zhaotong City, Yunnan Province

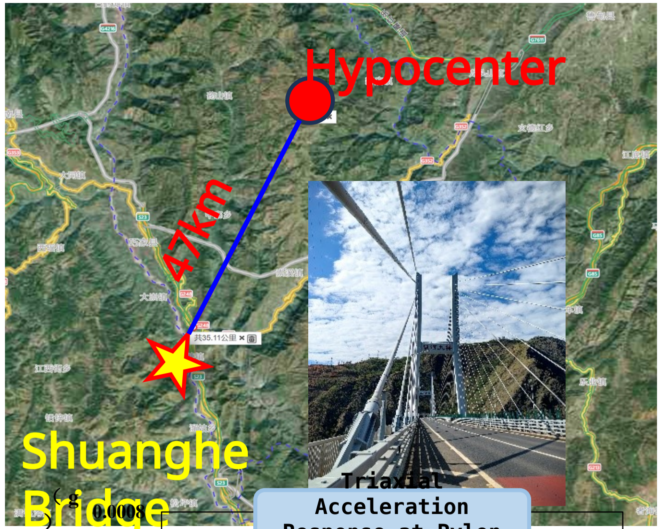

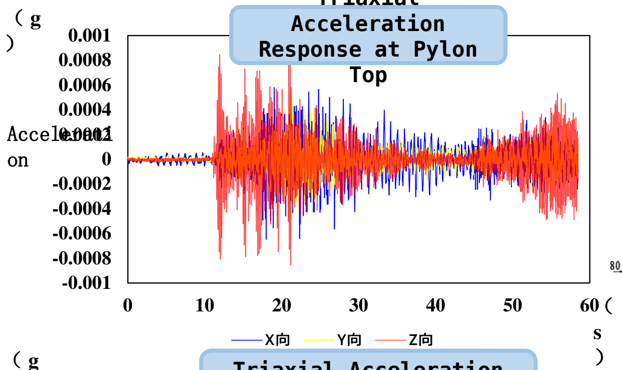

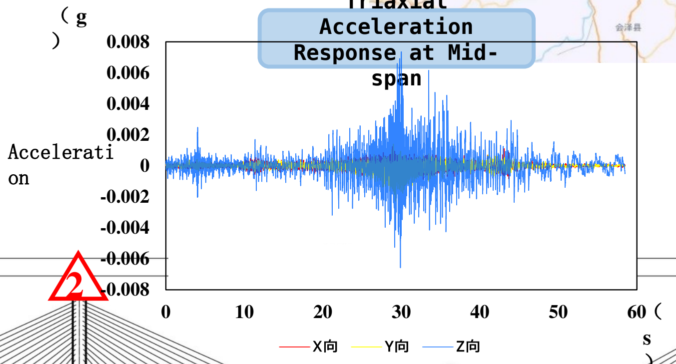

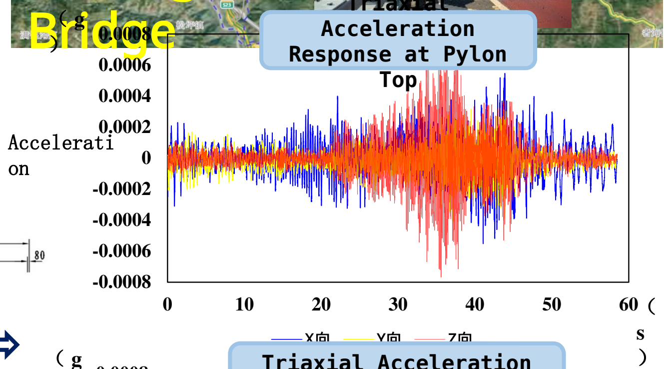

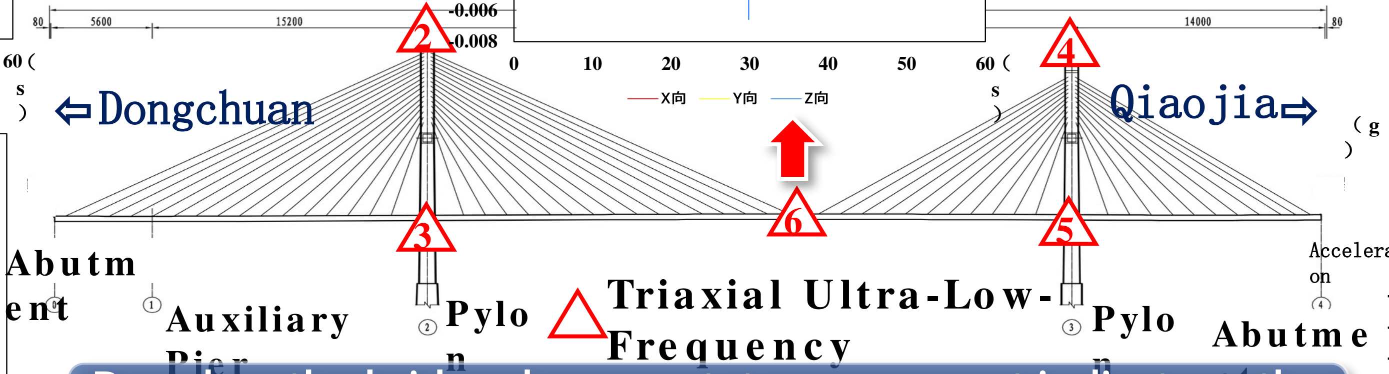

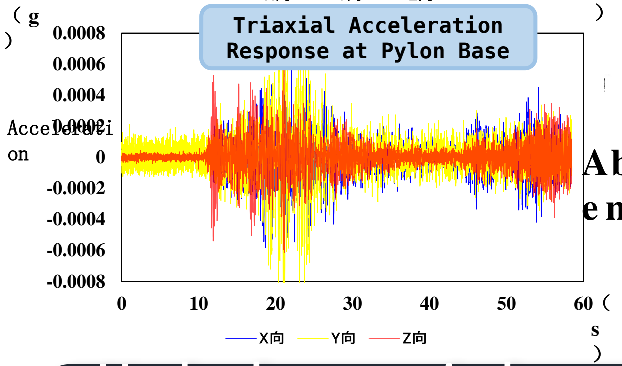

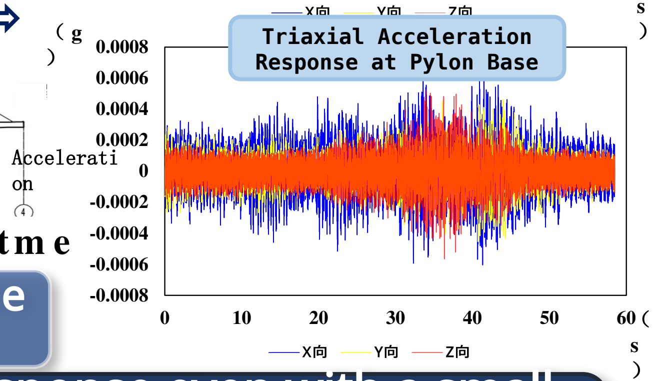

Based on the bridge damage state assessment indicators, the Shuanghe Bridge is in a damage-free state.

Under long-period ground motions, the bridge exhibits noticeable sway and response even with a small magnitude earthquake. Therefore, studying the bridge response to surface waves has both practical and engineering significance.

Basic Site Conditions

- Seismic Fortification Intensity: **Ⅷ**
- Characteristic Period of Response Spectrum: **0.45 s**
- Seismic Classification of Bridge Site: Class **A**
- Subsoil layers provide **reliable lateral restraint** to the pylon foundation.

Station Selection

- **Supplemental seismic data screening criteria**: similar site conditions, concentrated propagation azimuths
- Based on Chi-Chi earthquake records, select NEHRP Class C stations(**medium-stiff sites, Vs30≈360-760 m/s**) from the PEER database preferentially.

Station	Epicentral distance (km)	Vs30 m/s	NEHRP
TCU072	21.41	468.14	C
TCU045	77.44	704.64	C
TCU026	106.13	569.98	C
TAP052	148.33	433.88	C
TAP060	171.72	597.23	C

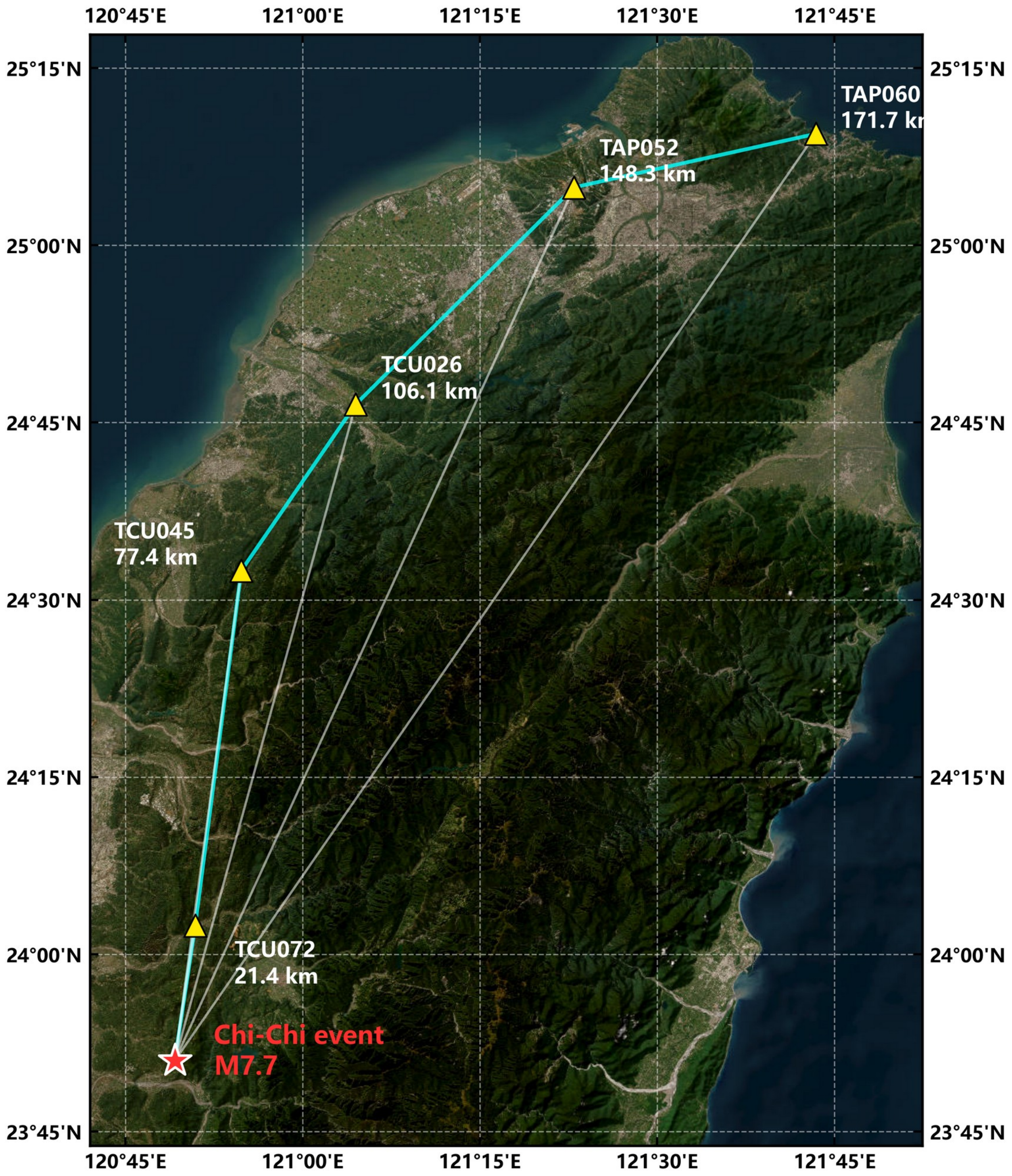

Acceleration Comparison

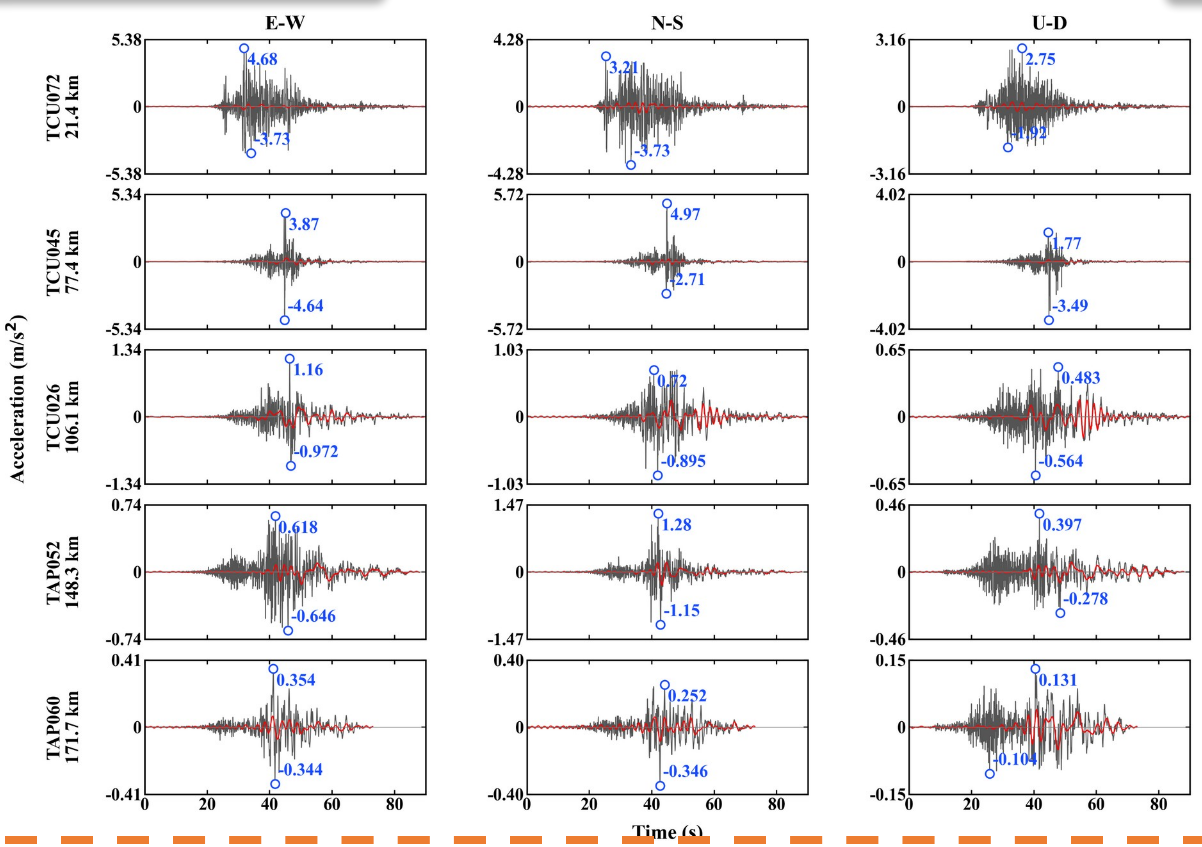

Displacement Comparison

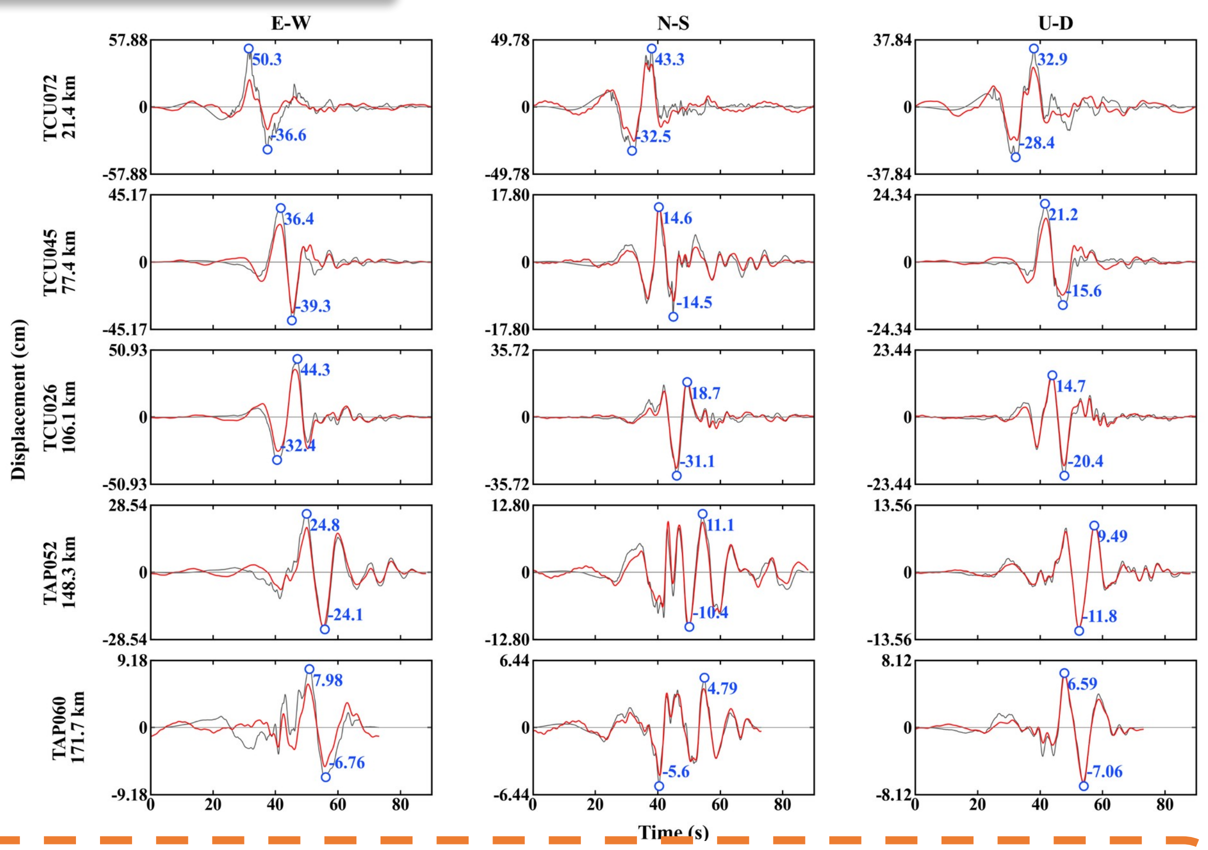

Response Spectra of Original Records

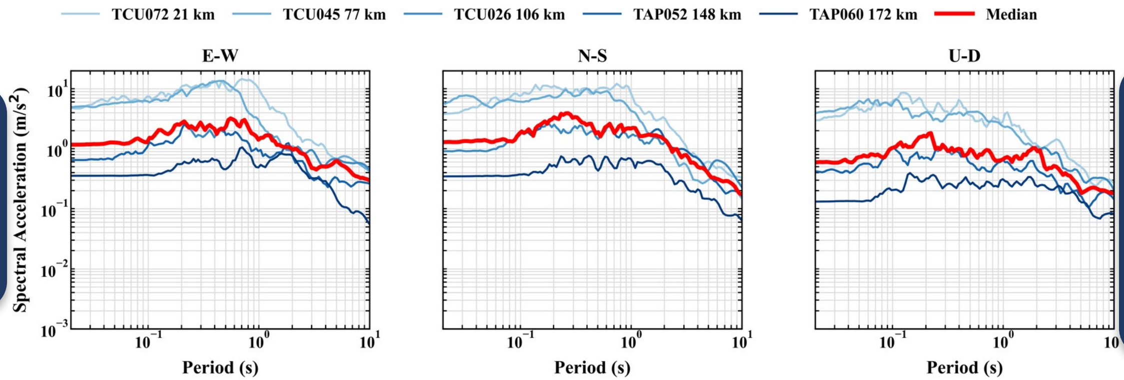

Response Spectra of Surface Wave Components

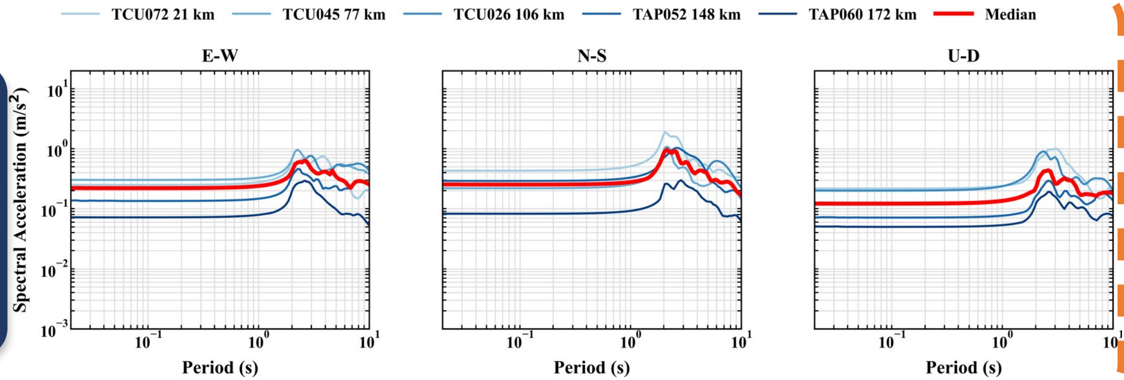

Displacement Response Ratio

- **Surface Wave Displacement Contribution： PCE/raw ratios differ markedly across stations.**
- **PCE (Extended Package: surface wave envelope)， full (raw: complete original waveform)**

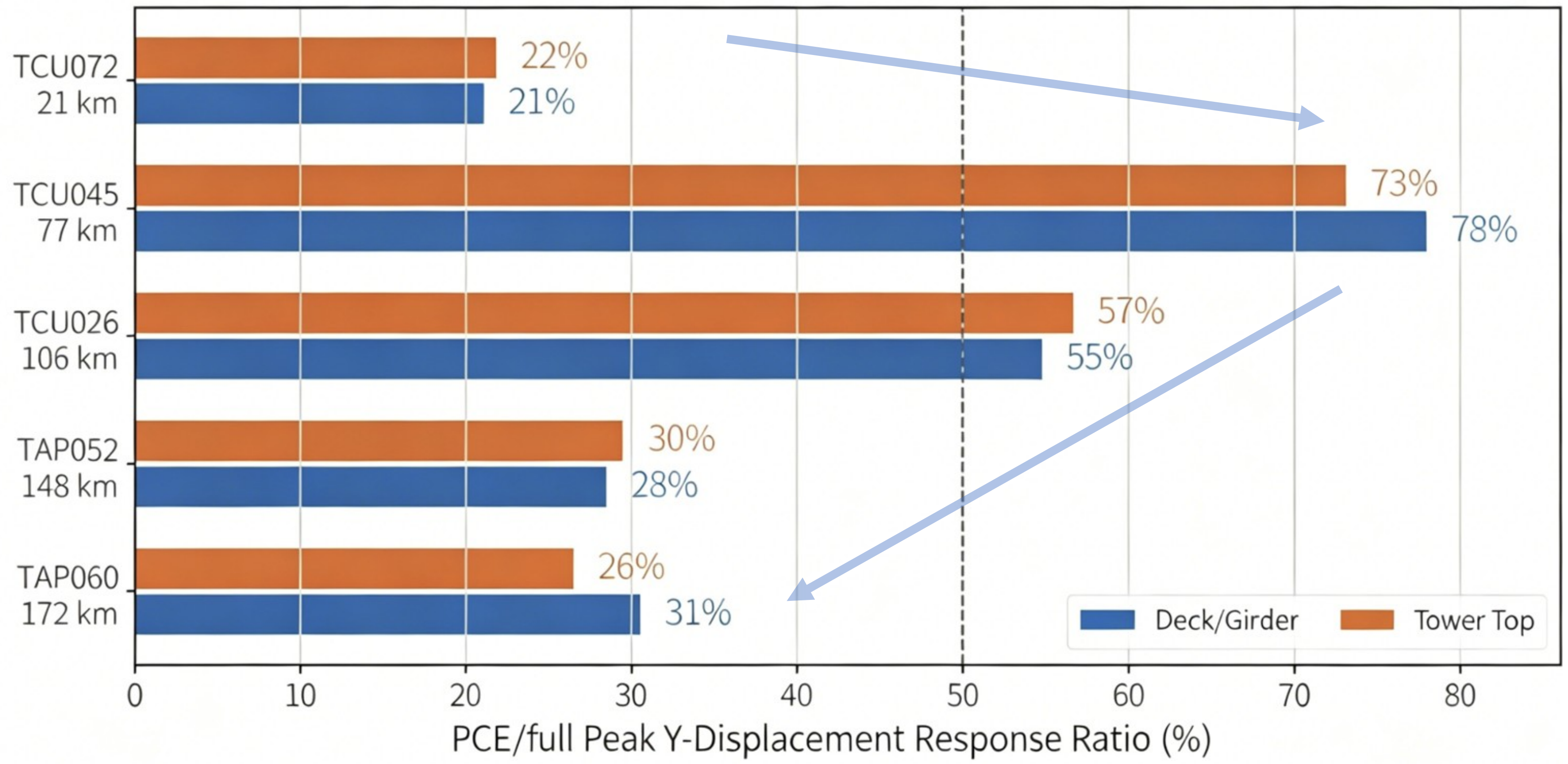

TCU045
Maximum Average Displacement Response Ratio
75.5%

TCU026 Deck / Tower Top
54.8% / 56.7%
Features both high proportional contribution and substantial absolute structural response

The surface-wave-induced displacement response ratio increases initially before decreasing as the source distance extends, which indicates that surface waves produce more remarkable seismic damage effects at sites of medium and long epicentral distances.

Analysis on Displacement and Displacement Ratio of Tower Top and Deck

➢ Comparison of Structural Responses of Tower Top and Deck/Girder under Full Input and PCE Surface Wave Excitation

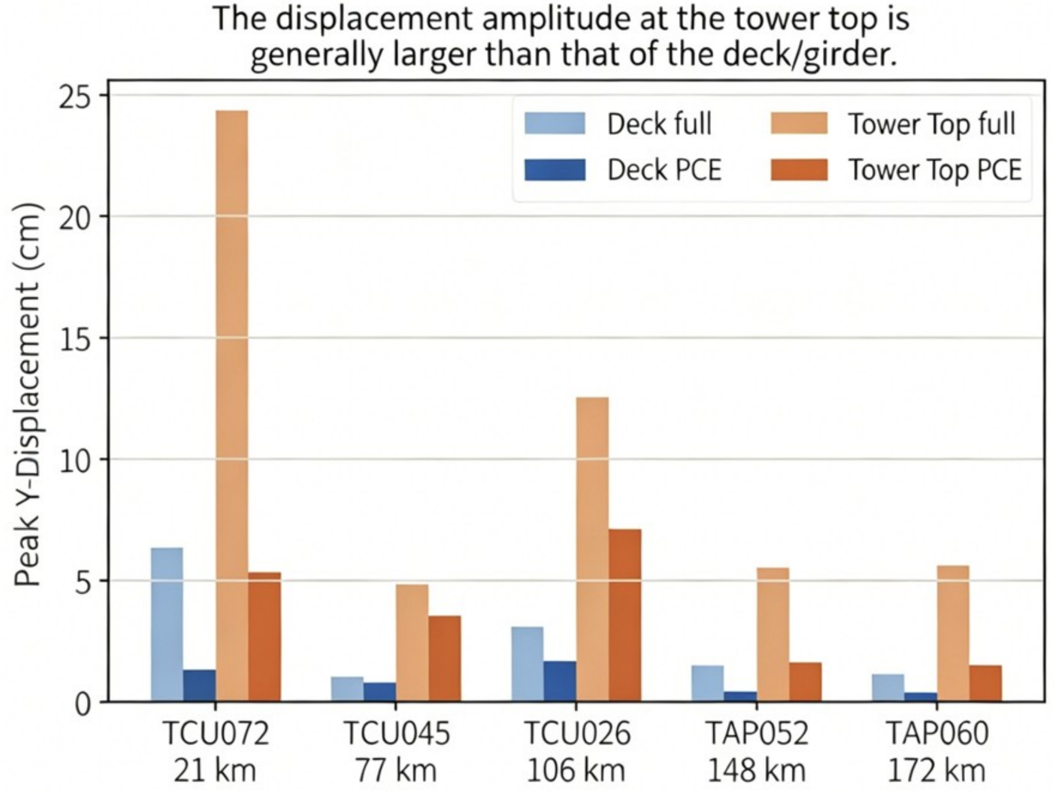

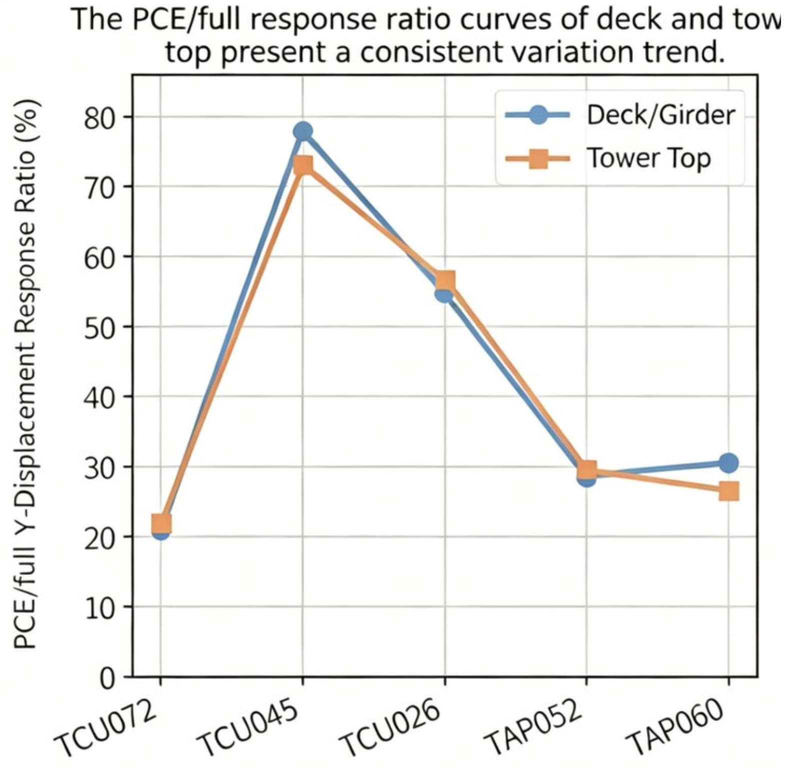

TCU026 Tower Top
12.6 cm full
7.1 cm PCE
56.7% PCE/full

TCU026 Deck/Girder
3.1 cm full
1.7 cm PCE
54.8% PCE/full

Tower top features larger displacement amplitude, while deck/girder and tower top share similar trends of PCE/full response ratio.

Amplitude Contribution of Surface Waves and Residual Components

➤ **To determine whether the full response is predominantly governed by the PCE surface wave component, the PCE surface wave and residual components are separately input into the bridge model, and their ratios of peak Y-direction displacement responses relative to the full input are compared.**

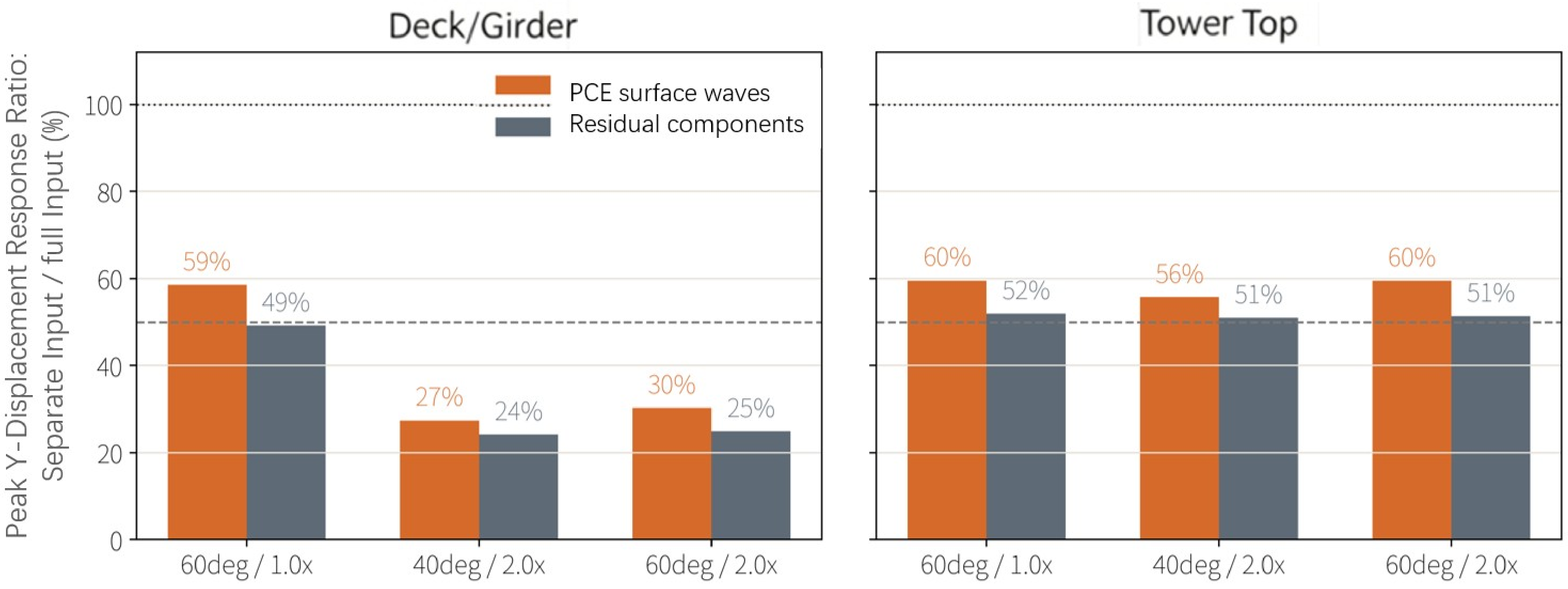

Peak Time History of Surface Waves and Residual Components

- To further identify the action mechanism of each wave component, the arrival instants of peak Y-direction displacements at the bridge deck/main girder and tower top under separate inputs of PCE surface waves and residual components are compared.

Arrival Time of Peak Response for Residual Components   Arrival Time of Peak Response for PCE Surface Waves

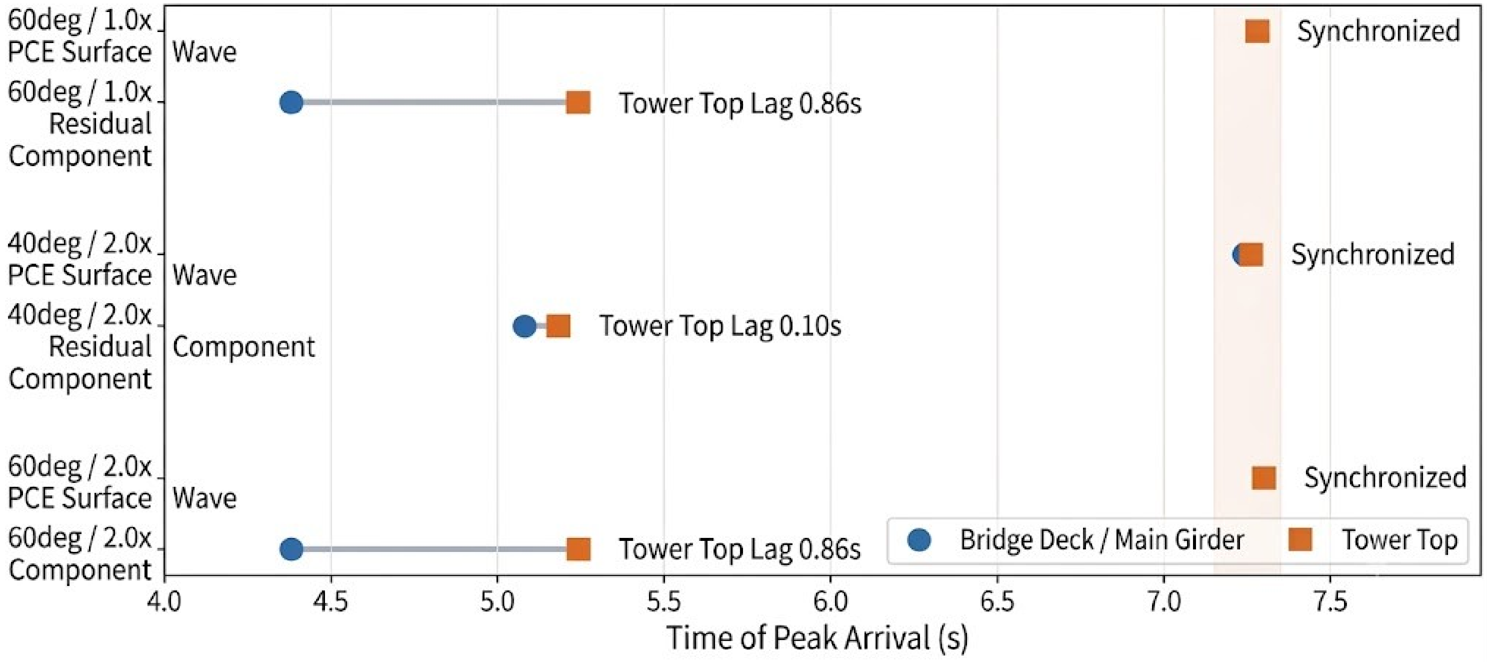

- Surface waves arrive later, and their peak arrival times are consistent with practical conditions.
- Residual components induce a phase difference between the tower top and bridge deck, which imposes substantial influences on isolation bearings and drives the bearings into a nonlinear state. This observation coincides with the bearing nonlinear behavior identified in the foregoing amplitude sensitivity analysis.
- PCE surface waves predominantly trigger global drift of the bridge structure and exert remarkable effects on bridge piers.

06 | Summary

- This study focuses on the influence of **long-period surface waves** on the **structural response** of **long-span flexible bridges**, establishing a complete research workflow **covering seismic record selection, surface wave component extraction, bridge dynamic response calculation**, and comparative analysis of results.
- Taking the **Shuanghe Bridge** as a case study of a long-span flexible bridge, and combining **with Chi-Chi earthquake station records**, the analysis preliminarily shows that long-period surface waves can significantly affect the **transverse displacement response** of long-span bridges, which has engineering significance for further research.
- The effects of **surface wave components** and **residual components** on structural response are different: surface waves are more likely to excite **global low-frequency synchronous responses**, while residual components may affect local components or different response stages. Therefore, the effect of surface waves should be regarded as a complex **ground motion-structure coupling problem**, rather than a simple **input decomposition problem.**
- This study has formed a preliminary evidence chain and **technical framework** for subsequent in-depth analysis, which can provide a reference for the evaluation of **long-period ground motion effects**, selection of **ground motion inputs**, and **seismic response analysis** of long-span flexible bridges.

Thanks for your attention!

WANG Tao, CHEN Jie, WANG Haiyun

Institute of Engineering Mechanics, China Earthquake Administration

June 6, 2026
ChangSha, China